Published in final edited form as:
Int J Cancer. 2010 May 15; 126(10): 2282–2295. doi:10.1002/ijc.24918.

Identification of ATP Citrate Lyase as a Positive Regulator of Glycolytic Function in Glioblastomas

Marie E. Beckner[1,+], **Wendy Fellows-Mayle**[2], **Zhe Zhang**[3,++], **Naomi R. Agostino**[2], **Jeffrey A. Kant**[1,4], **Billy W. Day**[3], and **Ian F. Pollack**[2,5]

[1]Department of Pathology, University of Pittsburgh, Pittsburgh, PA, 15213.

[2]Department of Neurological Surgery, University of Pittsburgh, Pittsburgh, PA, 15213.

[3]Department of Pharmaceutical Sciences, University of Pittsburgh, Pittsburgh, PA, 15213.

[4]Department of Human Genetics, University of Pittsburgh, Pittsburgh, PA, 15213.

[5]Children's Hospital of Pittsburgh, University of Pittsburgh, Pittsburgh, PA, 15213.

Abstract

Glioblastomas, the most malignant type of glioma, are more glycolytic than normal brain tissue. Robust migration of glioblastoma cells has been previously demonstrated under glycolytic conditions and their pseudopodia contain increased glycolytic and decreased mitochondrial enzymes. Glycolysis is suppressed by metabolic acids, including citric acid which is excluded from mitochondria during hypoxia. We postulated that glioma cells maintain glycolysis by regulating metabolic acids, especially in their pseudopodia. The enzyme that breaks down cytosolic citric acid is ATP citrate lyase (ACLY). Our identification of increased ACLY in pseudopodia of U87 glioblastoma cells on 1D gels and immunoblots prompted investigation of *ACLY* gene expression in gliomas for survival data and correlation with expression of *ENO1*, that encodes enolase 1. Queries of the NIH's REMBRANDT brain tumor database based on Affymetrix data indicated that decreased survival correlated with increased gene expression of *ACLY* in gliomas. Queries of gliomas and glioblastomas found an association of upregulated *ACLY* and *ENO1* expression by chi square for all probe sets (reporters) combined and correlation for numbers of probe sets indicating shared upregulation of these genes. Real-time quantitative PCR confirmed correlation between *ACLY* and *ENO1* in 21 glioblastomas ($p < 0.001$). Inhibition of ACLY with hydroxycitrate suppressed ($p < 0.05$) *in vitro* glioblastoma cell migration, clonogenicity and brain invasion under glycolytic conditions and enhanced the suppressive effects of a Met inhibitor on cell migration. In summary, gene expression data, proteomics and functional assays support ACLY as a positive regulator of glycolysis in glioblastomas.

Keywords

Glioblastoma; ATP citrate lyase; glycolysis; cell migration; invasion

Corresponding author and provider of reprints: Marie E. Beckner, MD, Department of Pathology, Room C2-26, Molecular Pathology Laboratory, Louisiana State University HSC - Shreveport, 1541 Kings Highway, Shreveport, LA 71130, Ph: (318) 675-7732, FAX: (318) 675-8395, mbeckn@lsuhsc.edu.
[+]Currently in the Department of Pathology, Louisiana State University Health Sciences Center - Shreveport, Shreveport, LA
[++]Currently in the Department of Biochemistry, University of Missouri, Columbia, MO

Brief overview: Cytoplasmic citric acid is a known negative regulator of glycolysis and is susceptible to cleavage by ATP citrate lyase (ACLY). Our initial identification of increased levels of ACLY in glioblastoma pseudopodia prompted studies that established ACLY as a positive regulator of glycolysis in glioblastoma cells.

Introduction

Glioblastoma (glioblastoma multiforme or Grade IV/IV astrocytoma) is a deadly, highly invasive type of brain tumor that responds poorly to conventional therapies. Glioblastoma cells thrive despite an irregular blood supply and a frequently hypoxic microenvironment. Compensatory mechanisms, including glucose uptake and glycolytic activity, are increased in these tumors (1,2,3). Our previous studies demonstrated that glioblastoma cells have sufficient glycolytic capacity to support tumor cell migration without mitochondrial participation (4,5). On 2D gel analysis of protein lysates, enolase and other glycolytic enzymes were found to be increased within glioma pseudopodia, suggesting glycolytic support of the leading edge during cell migration (6)..

In order to identify key proteins involved with metabolic adaptations during migration, glioblastoma pseudopodia were analyzed on 1D gels which enables the evaluation of proteins beyond the size range of our previous 2D gel-based studies. Identification of increased ATP citrate lyase (ACLY), a 121 kDa enzyme in pseudopodia of glioblastoma cells, suggested consideration of increased ACLY as a potential adaptation in glioblastoma cells that disconnect from the vasculature during invasion. ACLY's cleavage of cytosolic citric acid (8), released from mitochondria or transferred across plasma membranes, suggests a role for ACLY in regulating glycolysis. Hypoxia and ischemia potentially induce accumulation of metabolic acids by production and lack of systemic removal. Also, uptake of cytosolic citric acid by tricarboxylic transporters on mitochondria is diminished during hypoxia (9). Therefore, diminished cleavage by ACLY allows cytosolic citric acid to inhibit phosphofructokinase 1 and other glycolytic enzymes (10–12), especially when cells are sensitized by hypoxic and ischemic stress. Although ACLY is better known for its role in production of lipids in normal conditions, its control of citric acid levels in the cytoplasm of glycolytic tumor cells may well provide a key adaptation during invasion when cells are more reliant on glycolysis.

Clinical and functional data regarding a metabolic role for ACLY in these tumors were obtained. Queries of the NIH's REMBRANDT database for brain tumors (7) correlated *ACLY* gene expression with patient survival and co-expression of *enolase 1* (*ENO1*) in their tumors. Real-time quantitative (RQ) PCR was performed on additional tumors to further examine gene expression.

The role of ACLY in cells under glycolytic conditions was investigated in cell migration and other functional studies using inhibitors of ACLY. Effects of inhibitors on migrated cells, quantified in Boyden chambers, included effects on their pseudopodia. The deformation and translocation of cells through filters in these assays requires energy so that migration with mitochondrial inhibition reflected the cells' reserve glycolytic capacity. Our earlier studies had shown that equal numbers of glioblastoma cells migrated under glycolytic and normal conditions (5). Dependence on real-time production of energy rather than energy stored as creatine phosphate characterizes high grade astrocytomas (13) and simplifies the identification of effects on specific energy production pathways.

In this study, the differential effects in functional assays resulting from inhibition of ACLY in tumor cells, with and without exposure to glycolytic conditions, confirmed ACLY's role in protecting glycolysis. In our model, migration of glioblastoma cells was stimulated to enhance ATP production in normal and glycolytic conditions. Both serum and hepatocyte growth factor (HGF) or scatter factor, a known motogen (14), were used as chemoattractants when inhibitors of ACLY, hydroxycitrate and radicicol (15), were tested in assays. The results of functional assays coupled with gene expression and survival data suggest that ACLY is a promising target for inhibition of glioma invasion.

Materials and Methods

Materials and cell culture

All materials were obtained from Sigma (St. Louis, MO, USA) unless otherwise stated. Stock solutions of radicicol, 17-allylamino-17-demethoxygeldanamycin (17-AAG) and SU11274 (EMD Biosciences, Inc., La Jolla, CA), a Met kinase inhibitor, were prepared in dimethylsulfoxide. Potassium/calcium hydroxycitrate (600 mg/g SuperCitriMax, InterHealth Nutraceuticals, Inc., Benicia, CA, USA) was solubilized in Minimal Essential Medium (MEM) (Cellgro Media Tech, Herndon, VA). Human U87 and LN229 glioblastoma cell lines (American Type Culture Collection, Manassas, VA) were maintained in MEM with 10% fetal bovine serum (FBS) (Invitrogen, Carlsbad, CA). Half volumes of media were changed 1 d prior to each assay to normalize the cells' metabolic state. Antibody to glyceraldehyde-3-phosphate dehydrogenase (GAPDH) was obtained from Abcam, Inc. (Cambridge, MA). Anti-phosphorylated(p) ACLY (serine 454), anti-HSP90, and anti-Met (25H2) were obtained from Cell Signaling Technology (Beverly, MA). Horseradish peroxidase-labeled anti-mouse and anti-rabbit secondary antibodies were obtained from Kirkegaard & Perry Laboratories (Gaithersburg, MD). Protein standards, Multimark and Magic Mark, were obtained from Invitrogen.

Retrieval of pseudopodia from cultured cells

The method for obtaining pseudopodia from cells has been described in detail (6). Briefly, suspensions of 2×10^6/ml cells in MEM with 0.1% bovine serum albumin (BSA) were loaded in the upper wells of four-well Boyden chambers (Neuro Probe, Gaithersburg, MD) that were assembled with 0.01% porcine gelatin-coated, polycarbonate filters (Neuro Probe) containing pores, 1– or 3–μm diameter × 9-μm in length, to separate the upper and lower wells (Fig. 1*a*). The lower wells contained MEM with 0.1% BSA and chemoattractants, 2.5 ng/ml HGF and 0.1–1% FBS. Chambers were incubated at 37°C in 5% CO_2 for 6 h. Filters were removed, fixed in 100% methanol for 15 sec and placed on glass slides with migrated pseudopodia on their bottom surfaces. Unmigrated cells were very gently wiped completely from the top surface of the filter with large Kimwipes or cotton swabs using as little pressure as possible. Fresh Kimwipes were then pressed firmly on the filter for 30 sec to force adherence of pseudopodia to the glass (Fig. 1*b*). The filters were peeled from the slides leaving pseudopodia on the glass (Fig. 1*c* and *d*). If pseudopodia were not obtained with the first attempt, the filter was resubmerged in methanol for 5 sec and the process was repeated using a new glass slide. Yields were often scant and visualized best with the slide held against a dark background. Microscopy of Diff-Quik stained slides treated in a parallel fashion for harvesting pseudopodia confirmed the absence of nuclei in pseudopodial material for each cell line. Whereas filters with 3 μm pores worked well for U87 cells, cell lines with smaller size cells required filters with 1 μm pores. Pseudopodia on slides were stored at −80°C, batched and solubilized in lysate buffer consisting of 1.6 mM 4-(2-hydroxyethyl)piperazine-1-ethanesulfonic acid, pH 8.0, containing 6 M urea, 4% 3-[(3-cholamidopropyl)dimethylammonio]-1-propanesulfonate, 2 M thiourea and 20 mM dithiothreitol. Unmigrated cells, mostly whole cells, were allowed to adhere to filters in separate chambers and were transferred to glass slides as described above with transfer of the unmigrated cells to glass. Protein concentrations in the lysates were determined with the Bradford assay (Coomassie Plus Protein Reagent, Pierce, Rockford, IL).

Retrieval of pseudopodia from primary glioblastoma cells

Permission was obtained from the University of Pittsburgh's Institutional Review Board (IRB) for retrieval of pseudopodia from clinical specimens. Our method has been described (16). Briefly, after sufficient tissue for a diagnosis was obtained, the solid region of a glioblastoma was debulked with an ultrasonic suction aspirator (Integra Neurosciences,

Plainsboro, NJ) that generated a tumor cell suspension in saline and blood. The specimen was examined on smears to verify purity of the tumor sample. Only anaplastic cells with glial fibrils typical of glioblastoma cells, erythrocytes, and occasional fragments of blood vessels were seen. The specimen was then centrifuged (5 min, 500 rpm) and the loosely pelleted tumor cells were loaded in Boyden chambers for retrieval of pseudopodia as described above.

One-dimensional gel electrophoresis of pseudopodia and unmigrated cells

Lysates of pseudopodia and unmigrated cells, equalized for total protein content (10 μg per lane) or with GAPDH, as indicated, were electrophoresed in separate lanes of 10% polyacrylamide gels under reducing conditions. It has been shown that protein and RNA expression of *GAPDH* remain stable in glial cell lines and tumors regardless of metabolic stress (17). Each gel was stained with Coomassie blue (Novex Colloidal Blue Stain Kit, Invitrogen) and destained with tap water. Protein standards were loaded as 8 μg per lane in each gel.

Protein Identification

As previously described (18), gels were submitted to the Michigan Proteome Consortium, University of Michigan (Ann Arbor, MI). Robotic collection, destaining and trypsin treatment of plugs from the gels were performed on Coomassie blue-stained bands that were increased in lysates of U87 pseudopodia compared to unmigrated cells. Following trypsin digestion, peptides derived from the 120 kDa band were analyzed with matrix-assisted laser desorption ionization time-of-flight mass spectrometry (MALDI-TOF-MS) in 4700 and 4800 Proteomics Analyzers with TOF/TOF optics (Applied Biosystems, Foster City, CA). Optimized spectra calibrated by trypsin autolysis peptide ion signals were used to generate peak lists. Peptide mass fingerprint searches with the Mascot (http://www.matrixscience.com) program and the MS-Fit program (http://prospector.ucsf.edu) were used for protein identification utilizing NCBI and SwissProt databases. The search parameters have been described (18). Protein identifications were accepted when observed and predicted M_r's were consistent and scores indicated nonrandom identifications at the $p < 0.05$ level of significance. For immunoblotting of pseudopodia and unmigrated cells, gel contents were transferred onto polyvinylidene difluoride membranes (Invitrogen), blocked (Detector Block, Protein Detector Western Blot Kit Lumi-GLO System, Kirkegaard & Perry Laboratories, Gaithersburg, MD) and reacted with primary antibodies, anti-pACLY (1:250), anti-GAPDH (1:1000) and anti-HSP90 (1:333). Secondary antibodies, horseradish peroxidase-labeled anti-mouse and anti-rabbit (1:1000) were used for anti-pACLY, and anti-GAPDH and anti-HSP90, respectively. Immunoreactive bands were visualized via chemiluminescence and the blots were scanned.

Queries of the REMBRANDT database

Gene expression (Affymetrix) and Kaplan-Meier survival data for *ACLY* and the gene encoding enolase, *ENO1*, were queried online in 2008 – 2009, by following the site's instructions for "simple search" (7). Initially, queries were based on averages of the probe sets (termed reporters or locaters), the only data available prior to 2009. The database of 179 gliomas in May, 2008, had been expanded to 201 gliomas by February, 2009. Newer versions of REMBRANDT included results from separate probe sets, four and five for *ACLY* and *ENO1*, respectively. These results are available on pull-down menus under the button for "reporters" and were used in this study to investigate relationships between *ACLY* and *ENO1* with *chi square* and correlation coefficient (*r*) analyses.

Real-time quantitative PCR (RQ-PCR)

With the University of Pittsburgh IRB's approval, RNA expression was studied in frozen samples of glioblastomas resected from 24 patients (average age of 62.9 yr, range of 19 – 81 yr) provided by the University of Pittsburgh Brain Tumor Tissue Bank. Nucleic acid extraction, either an automated method via MagNA Lyser, MagNA Pure Compact, and MagNA Pure Compact Nuclei Acid Isolation Kit I (Roche Diagnostics Corp., Indianapolis, IN) or a manual method (pulverization of frozen tissue into lysate buffer, RNAeasy Plus Micro Kit (Qiagen, Valencia, CA) and homogenization with a syringe and needle) were followed by RNA purification with the RNAeasy Plus Micro Kit. For expression analysis, cDNAs were prepared from purified RNA of the tumor samples and pooled reference non-malignant brain tissue samples obtained from 23 adults, average age of 68.3 yr, range of 23 – 86 yr (First Choice Human Brain Reference RNA, Ambion Applied Biosystems, Austin, TX). Sufficient RNA for further analysis was obtained from 22 of the 24 frozen tumor samples. The cDNAs in tumor and reference samples were analyzed in triplicate wells for expression of *ACLY*, *ENO1*, *ACTB* (encodes actin B) and *GAPDH* and human genomic DNA and reverse transcription controls were tested in single wells of the same 96-well plates (Custom R^2 PCR Arrays, SuperArray Biosciences, Corp., Frederick, MD). Primers for the genes and controls (pre-loaded on the custom plates) had been tested for specificity and equal efficiencies of amplification by the manufacturer and were confirmed by dilution curves in our laboratory (not shown). The cDNA samples were loaded with RT^2 SYBR Green/ROX PCR Master Mix (SuperArray Biosciences Corp.). Amplification with data retrieval was performed on the ABI 7500 Prism Thermocycler System (Applied Biosystems, Foster City, CA). The delta-delta crossing threshold (ddC_t) method was used to determine fold increases of each gene of interest in the tumor samples compared to the non-malignant reference sample with the averaged values of two house keeping genes used for normalization. The dC_t for each gene in an assay equaled C_t (gene of interest) – average C_t (house keeping gene). The ddC_t for each gene equaled dC_t (tumor sample) - dC_t (reference non-malignant brain sample). The fold-change for each gene from the normal reference sample to the tumor sample was calculated as 2^{-ddCt} (the negative ddC_t exponential function of 2).

Cell migration

Confluent cells were trypsinized and allowed to recover in MEM containing at least 10% FBS for 2 h at 37°C. Incubation in MEM lacking phenol red optimized recovery. Cells, 1.5×10^6/ml, in MEM (with phenol red), with 0.1% BSA were loaded in the upper wells of modified Boyden chambers assembled with gelatin-coated filters (8-μm pores). The lower wells contained MEM (with phenol red), 0.1% BSA and chemoattractants, 2.5 ng/ml HGF and 1% FBS. The chambers were incubated at 37°C for 5–6 h in 5% CO_2. Glycolytic conditions were generated by suppression of cytochrome oxidase in mitochondrial respiration with 27 mM NaN_3. Our earlier study demonstrated that 10 – 50 mM NaN_3 did not inhibit cell migration under normoxic or hypoxic conditions (5). Multiple studies, including investigations of astrocytic cells, have used sodium azide to generate chemical hypoxia (19–29). The inhibitors, hydroxycitrate, radicicol, 17-AAG and SU11274, were added in the concentrations indicated. Control wells included the highest concentrations of vehicle used in the dose-response curves. Upon completion of the assays, the migration filters were stained with Diff Quik (Fisher Scientific, Pittsburgh, PA) and analyzed. The pellets of migrated cells were digitized using a transparency scanner (Epson Perfection 4990 PHOTO, Epson America, Long Beach, CA) and densitometry software (UN-SCAN-*It* gel, Silk Scientific, Orem, UT) with correction for background density of the filters. Results of migration assays (at least three assays with four replicates each) were stated as percent of control migration (no inhibitory drugs) under either normal or glycolytic (mitochondria

inhibited) conditions. Analysis of cell viability at 6 h, as indicated by trypan blue exclusion, was performed with light microscopy.

Clonogenic assays

Suspended U87 cells, treated with NaN_3 (27 mM), hydroxycitrate (3 mM), both NaN_3 and hydroxycitrate, or no inhibitors for 5 h in MEM (with phenol red) containing 1% FBS and 0.1% BSA, were centrifuged (5 min, 500 rpm), resuspended in MEM containing 10% FBS and plated, 250 cells per well, on six-well plates. After 10 d in culture the cells were stained with Diff Quik and their colonies were manually counted in each well.

Cell invasion of rat brain slices

Brains of rats (Harlan Sprague-Dawley) were sliced in a rat brain sagittal matrix (Kent Scientific Corp., Torrington, CT). The slices were transferred to six-well plates coated with Matrigel (BD Biosciences, Bedford, MA). Sterile transfer pipets with 0.5 cm diameter stems (Fisher Scientific) were cut into 1 cm segments with inclusion of a flared end for each so that funnels were formed. Stems of the funnels were used to punch out 1 × 5 mm discs of fresh brain tissue resting on Matrigel. The funnels containing wedged brain slices (1 mm thick) were placed with their flared ends upright on 8-chamber glass culture slides (BD Biosciences). Trypsinized U87 cells, recovered in phenol red-free MEM containing 20% FBS for 2 h at 37°C, were labeled with a red fluorescent dye, the chloromethyl derivative of 1,1'-dioctadecyl-3,3,3',3'-tetramethylindocarbocyanine (CM-DiI Cell Tracker (Invitrogen). Cells were centrifuged, resuspended at 0.5×10^6/ml in Matrigel and then 50,000 cells (100 μl) were immobilized on the rat brain slices wedged in funnels as Matrigel solidified. A two well system with gradients was created by adding MEM (with phenol red) on top of the cells embedded in the layer of solidified Matrigel overlying the brain slice in the funnel, checking for leakage, and then adding media with chemoattractants (5 ng/ml HGF and 5% serum) outside the funnel sitting in a plate well. Hydroxycitrate was added to both sides of the brain slices as indicated. After 7 d at 37°C in 5% CO_2, funnels with brain sections were fixed overnight in 10% formalin and the bottom edges of tissue were inked. Routine hematoxylin and eosin (H&E) sections were prepared. The bottom edges of brain slices were examined to detect tumor cells labeled with CM-DiI in comparison with host cells seen only in the H&E sections. Cell counts were obtained using a BHS-RFC reflected light fluorescence attachment (Olympus Corp., Center Valley, PA) with the appropriate filter for CM-DiI.

Statistical methods

Chi-square analysis was performed with one degree of freedom in two-x-two tables. Correlation coefficients, trendlines and the levels of significance for regression in the REMBRANDT expression and RQ-PCR data were also obtained. Significance of correlation coefficients obtained from REMBRANDT data was determined by the *p* values of the *student t* statistics. Regression modeling was performed in S-Plus on RQ-PCR data (v. 7.0 for Windows, Insightful Corp., Seattle, WA) to derive best slope-parameter estimates between *ENO1* and *ACLY* expression results. Outlier detection was based on detection of a difference greater than three SD from the average for the other residuals in the regression model. The means with 95% confidence intervals (CIs) and significant differences ($p < 0.05$) with two-tailed *student t* tests were determined for tumor and non-malignant reference brain tissue samples in expression studies and for tumor cells in functional assays, with and without exposure to inhibitors or glycolytic conditions. In the functional studies each data point was converted to the percent of the average control value (cells with no inhibitor) obtained in the same assay to correct for assay-to-assay variation. Concentrations of inhibitors (IC_{50}'s) that suppressed cell migration to 50% of levels exhibited by control cells (no inhibitors), were derived from equations for trendlines of the dose curves (Microsoft Office Excel 2003). Data points greater than 3 SD from the mean were treated as outliers.

Results

Identification of ACLY in lysates of glioblastoma pseudopodia

Unmigrated U87 cells and their pseudopodia were harvested as lysates from filters containing 3- and 1-μm diameter pores. The lysates were equalized for total protein, electrophoresed, stained with Coomassie blue and visually compared. A 120 kDa band that was increased in the U87 pseudopodia (Fig. 2*a*) was excised and digested with trypsin. It was identified by mass spectrometry (MS) as ACLY isoform 2 (*Homo sapiens*, Accession No. 38569423, M_r = 120608, protein score = 165 with CI% = 100 and total ion score = 130 with CI% = 100) with two peptides, R.GGPHYQEGLR.V (observed 1090.50, missed cleavage = 0, ion score = 39, CI% = 98.955, Mascot, S/N = 111, resolution = 7181) and K.WGDIEFPPPFGR.V (observed 1417.67, missed cleavage = 0, ion score = 53, CI% = 99.959, Mascot, S/N = 153, resolution = 12071). The MALDI-TOF/TOF-MS/MS spectrum for an ACLY peptide is shown (Fig. 2*b*). Identification of the lower molecular weight band (68 kDa) as BSA has been previously described in pseudopodia of glioblastoma cells (18). Lysates of pseudopodia and unmigrated glioblastoma cells were immunoblotted to compare levels of pACLY. Levels of HSP90 were also compared. Pseudopodia formed by U87 cells on filters with 3- and 1–μm diameter pores demonstrated 3.5-fold and 2.4-fold elevations of pACLY (125 kDa), respectively, compared to unmigrated cells. The loading control was GAPDH and loading equalized by total protein was also similar. In contrast, the levels of HSP90 (92 kDa) in U87 pseudopodia (3- and 1-μm) fell by 46% and 39%, respectively, compared to unmigrated cells. The levels of GAPDH (36 kDa) in pseudopodial lysates (3- and 1-μm diameters) were 91% and 95%, respectively, of the levels in unmigrated cell lysates (Fig. 2*c*). The immunoreactive band that reacted with anti-pACLY in pseudopodia formed by aspirated primary glioblastoma cells had a lower M_r than intact pACLY. However, its size (53 kDa), was the same as a predicted digestion product (DP) of ACLY that is known to retain activity (30,31). The levels of pACLY-DP were 4.7-fold greater in primary tumor cell pseudopodia than in unmigrated cells. In contrast, the levels of HSP90 in the primary cell pseudopodia were much lower, only 7% of the unmigrated cells. Strong positive staining of the pseudopodial lysate on this immunoblot for glial fibrillary acidic protein has been previously shown (16). Loading was approximately equalized by GAPDH. Levels of GAPDH in lysates of primary cell pseudopodia (limited material available) were 84% of those in unmigrated cells (Fig. 2*d*). Only the 36 kDa band of GAPDH was used for equalizing loading of viable cellular material. Results with loading equalized by reactivity for anti-β-actin also demonstrated increased ACLY in the pseudopodia (not shown).

Queries of the national REMBRANDT database of brain tumors

Expression of *ENO1*, the gene encoding enolase is a variably expressed glycolytic enzyme, was used as an indicator of glycolytic activity. Affymetrix gene expression data with survival information was available from multiple institutions in the NIH's REMBRANDT database of brain tumors (7). The levels of gene expression for *ACLY* and *ENO1* were increased at least two-fold in 85 (42%) and 96 (48%), respectively, of 201 gliomas from multiple institutions when results of all probe sets (reporters) available in the database were combined for each gene. The gliomas included a subset of 109 glioblastomas. The survival on Kaplan Meier plots of patients with gliomas showed a significant adverse association with increased expression of *ENO1* as determined using five probe sets (reporters) with *p* values that ranged from 6.0×10^{-4} to 0.0057 (Table 1, Column 4). Survival was also adversely associated with increased *ACLY* expression as assessed using four probe sets with *p* values that ranged from 8.0×10^{-4} to 0.018 (Table 1, Column 9). By *chi square* analysis, the association between increased expression of *ACLY* and *ENO1*, as indicated by all of probe sets collectively, was highly significant, $p = 3.85 \times 10^{-5}$ and $p = 0.00255$, in 201 gliomas and 109 glioblastomas, respectively. Correlation analysis was performed to

determine the relationship between increased gene expression for *ACLY* and *ENO1* as indicated by the number of probe sets indicating increased expression in the same tumors with zero to a maximum of four and five probe sets for *ACLY* and *ENO1*, respectively. The correlation coefficient, $r = 0.972$, for the number of Affymetrix and Unified Gene probe sets indicating at least two-fold increased gene expression for *ACLY* and *ENO1* in each glioma was highly significant with a two-tailed *student t* statistic of 9.248, $p < 0.0005$. In glioblastomas, $r = 0.990$, for the same relationship of *ACLY* and *ENO1* probe set results in each tumor with a two-tailed *student t* statistic of 15.692, $p < 0.00005$. The mean numbers of probe sets with 95% CI indicating increased expression of *ACLY* are graphed on the y axis against the numbers of probe sets indicating increased expression of *ENO1* in each glioblastoma on the×axis is shown in Fig. 3*a*.

Real-time quantitative PCR results

The relationship between *ENO1* and *ACLY* was then tested with another technique on a different set of glioblastomas that were surgically resected at the University of Pittsburgh. The expressions of *ENO1* and *ACLY* n 22 tumors obtained with RQ-PCR using the ddC_t method were examined with correlation analysis. Studies of the first six glioblastomas tested showed that normalization with averaged values of both housekeeping genes, *ACTB* and *GAPDH*, yielded comparable *r* values to using either housekeeping gene alone (not shown). The graphical results of the 22 glioblastomas tested indicated that there was one outlier that was discarded after examination of a best-fit regression model. The outlier was greater than three SD from the average residual value of the other data points. The 21 residual values remaining were approximately normally distributed (not shown). The value of *r* between *ACLY* and *ENO1* in 21 tumors was 0.756, a highly significant result with a two-tailed *student t* statistic of 5.05, $p < 0.0001$ (Fig. 3*b*). The best-fit regression model also indicated statistical significance of the relationship between between *ENO1* and *ACLY*, $p < 0.001$. The coefficients of variation for dC_ts of *ACLY* and *ENO1* in the reference sample (six assays) were 0.055 and 0.087, respectively. The average C_ts with 95% CIs for the human genomic DNA contamination control and reverse transcription control were 32.87 ± 0.29 and 21.67 ± 0.46, respectively, for the tumor samples and 32.86 ± 0.67 and 20.69 ± 0.67 for the reference samples, respectively, with no significant differences between the sample types, $p < 0.05$.

Suppression of cell migration with inhibition of ACLY by hydroxycitrate

A potassium/calcium salt of hydroxycitrate, a competitive inhibitor of ACLY (32), at a concentration of 0.3 mM suppressed U87 cell migration dependent on glycolytic ATP (mitochondria inhibited) but not under normal conditions when mitochondrial ATP could be generated (Fig. 4*a*). As a negative control, 0.3 – 3 mM potassium citrate did not have a suppressive effect on U87 cell migration in glycolytic or normal conditions and its slight suppression at 12 mM under glycolytic conditions was not significant (not shown). Glycolytic and normal migration of LN229 cells was suppressed at 3 and 24 mM hydroxycitrate, respectively (Fig. 4*b*). Under glycolytic conditions the IC_{50}'s for hydroxycitrate were 16.7 and 12.1 mM for U87 and LN229 cells, respectively. Cell viability was unaffected during the assays.

Suppression of cell migration with inhibition of ACLY by radicicol

Radicicol, an inhibitor of ACLY and HSP90, was tested under glycolytic and normal conditions. HSP90 is a chaperone for Met and other kinases and suppression of its activity can have widespread effects on cell migration. Migration of U87 cells in glycolytic and normal conditions was significantly inhibited by 17 μM radicicol (Fig. 5*a*). Migration of LN229 cells in both types of conditions was also suppressed by radicicol (Fig. 5*b*). In addition, 17-AAG, another inhibitor of HSP90 (33) whose effects on ACLY are unknown, significantly inhibited U87 cell migration in both conditions at 17 μM (not shown). LN229

cells in glycolytic conditions were also sensitive to 17 μM 17-AAG (not shown). The IC_{50}'s of radicicol and 17-AAG for U87 cells were 38.5 and 61.3 μM, respectively, under glycolytic conditions, and 53.2 and 93.3 μM, respectively, in normal conditions. The IC_{50}'s of radicicol and 17-AAG for LN229 cells were 20.8 and 39.3 μM, respectively, in glycolytic conditions, and 23.4 and 80.8 μM, respectively, in normal conditions. Cell viability was unaffected during the assays. Prior to the 5–6 h assays the glioblastoma cells were not pre-incubated with these drugs. The relatively high inhibitory amounts of 17-AAG required for the cell concentrations (2 million/ml) used in Boyden chambers with no pre-assay drug exposure were within the micromolar range required for high numbers of tumor cells in short chemotaxis assays (34).

Hydroxycitrate-enhanced suppression of cell migration by SU11274

Stimulation of Met enhances glioblastoma cell migration. Accordingly, the Met kinase inhibitor SU11274 (35–38), at 2.8 μM suppressed migration of U87 cells significantly ($p < 0.05$) in normal and glycolytic conditions. Significant suppression of glycolytic LN229 migration was achieved at comparable concentrations but normal (no mitochondrial inhibition) migration was resistant (not shown). When hydroxycitrate (3 mM) was combined with SU11274 (2.8 – 22.5 μM), a significant ($p < 0.05$) additive suppressive effect on glycolytic U87 cell migration resulted. In four assays under glycolytic conditions, the IC_{50} of SU11274 for U87 cells, 14.2 μM, was reduced to 7.47 μM when combined with 3 mM hydroxycitrate. The pellets of migrated cells are shown in Fig. 6*a* with the results graphically represented in Fig. 6*b*. SU11274's suppressive effect on LN229's glycolytic migration was not enhanced by 3 mM hydroxycitrate (not shown).

Suppression of clonogenic potential and brain slice invasion with inhibition of ACLY

Hydroxycitrate suppressed the clonogenic potential of glycolytic U87 cells. Test cells were exposed to 3 mM hydroxycitrate and glycolytic conditions (inhibition of mitochondria) for 5 h prior to being plated for 10 d of culture in two assays. Significant differences ($p < 0.05$) were detected when hydroxycitrate-treated cells were compared to cells unexposed to hydroxycitrate or NaN_3 (mitochondrial inhibitor) or to NaN_3 alone (Fig. 7*a*). In another type of functional assay, hydroxycitrate suppressed U87 cell invasion through tissue slices of rat brain maintained for 7 d in glycolytic conditions (NaN_3 present). The cells invaded brain slices in the presence of a chemoattractant gradient generated by 5 ng/ml HGF and 5% FBS. Significant suppression ($p < 0.05$) of invasion by 3 and 12 mM hydroxycitrate was 37% and 38%, respectively, compared with control (no hydroxycitrate) in three assays that are summarized in Fig. 7*b*. Two of the 12 data points obtained for 3 mM hydroxycitrate were outliers and were not included.

Discussion

After discovery of ACLY's increased distribution in glioblastoma pseudopodia, two glioblastoma cell lines were examined to determine the significance of ACLY's role in regulating tumor cells in glycolytic conditions. We previously identified glycolytic enzymes as the most prominent group of proteins increased in U87 pseudopodia on 2D gels, with enolase included among the increased glycolytic enzymes (6). ACLY is related to glycolysis via its breakdown of cytosolic citric acid. Brain tissue of suckling rats and cultured astrocytes are known to release citric acid from mitochondria (39,40,41). Also, an enhanced rate of citric acid release to the cytoplasm from mitochondria has been noted for poorly-differentiated versus well-differentiated hepatomas (42). Although studies on the release of citric acid from mitochondria have not been performed in astrocytic tumors, citric acid levels in brain tumors are higher than in non-malignant brain (43,44).

Others have reported that hypoxia, a glycolytic condition, stimulates glioblastoma cell migration (45,46) and it is well known that hypoxic tumor cells with increased glycolytic capacity resist many drugs (47–55). Glioblastomas commonly exhibit large areas of hypoxia *in situ*, with the potential for accumulation of intracellular metabolic acids, such as lactic and citric acid. Although increased levels of these acids should impair glycolysis, glioblastomas paradoxically upregulate the glycolytic pathway to levels that not only sustain viability but also promote profound invasiveness in an adverse environmental milieu. The rapid responsiveness of the glycolytic pathway (56) as well as its simplicity offer advantages to glioblastoma cells in harsh microenvironments provided it can be protected from acidosis. The simplicity of the glycolytic pathway compared to mitochondria represents a smaller collective target in regard to the numbers of proteins and genes that are affected by drugs, toxins, and genetic instability.

Therefore, enzymes and other proteins that protect glycolytic activity from acidosis need to be identified and investigated as targets to improve therapies of these invasive tumors. We previously investigated tumor cell metabolism of lactic acid, the inhibitory by-product of anaerobic glycolysis (5). Cytosolic citric acid also normally “brakes” glycolysis but its inhibitory effects appear to be negated when cleaved by ACLY, as illustrated in Fig. 8. This study demonstrated enhanced levels of ACLY in pseudopodia, decreased patient survival associated with increased expression of *ACLY* in brain tumors, co-expression of increased *ACLY* and *ENO1* and functional suppression of glioblastoma cells by a competitive inhibitor of ACLY, with specificity for glycolytic conditions. Thus, these results support ACLY as playing a protective role for the glycolytic pathway in glioblastomas. We hypothesize that ACLY’s well established role in lipid synthesis under normoxic conditions is not responsible for the effects of ACLY’s inhibitors that preferentially suppress glycolytic rather than normoxic cell migration.

Identification of proteins distributed to tumor cell pseudopodia should highlight those enzymes that play important roles in dynamic, energy-consuming cellular functions, such as migration. In that context, our detection of increased ACLY within pseudopodia of glioblastoma cells, including primary tumor cells, suggests that ACLY is important in promoting tumor invasion due to its protection of the glycolytic pathway in motile cellular extensions. Metabolism of citric acid via ACLY relieves inhibition of phosphofructokinase 1 and other glycolytic enzymes in tumor cells to putatively increase tolerance for ischemia. Suppression of ACLY inhibited cell migration under glycolytic conditions with no effect (or a much smaller one) on cell migration in normal conditions which supports a specific role for ACLY in protecting glycolysis.

Others have hypothesized that increased ACLY is necessary for the growth of tumor cells via production of acety-CoA for lipid synthesis so that inhibition of ACLY effectively blocks the growth of tumors (57). The production of acetyl-CoA via ACLY may also be involved in histone acetylation (58). Our 6 h migration studies were too short to be influenced by cell proliferation, and thus we do not address these roles for ACLY during normoxia. However, ACLY’s production of acetyl-CoA in normoxia may constitute another physiologically relevant advantage of targeting ACLY in metabolic tumor treatments. However, the brain is rich in lipids that are available to invasive tumor cells in either normal conditions or hypoxia. The brain contains 25% of the body’s cholesterol (59) and exogenous lipids are supplied from the bloodstream to the brain (60). In hypoxia the supply of extracellular lipids to invasive tumor cells may be crucial since acetyl-CoA metabolism for lipid synthesis is diminished. When ATP levels fall compared to AMP in hypoxic normal cells, AMP-activated protein kinase suppresses lipid synthesis from acetyl-CoA by inhibition of acetyl-CoA carboxylase and lowering its affinity for citrate, an allosteric activator (61). However, exogenous lipids can be delivered to hypoxic tumor cells *in vivo*

through the permeable blood brain barrier found in glioblastomas. Exogenous lipids (serum and BSA) were provided in these assays to support cell migration and to minimize synthesis of lipids as a variable. Pseudopodia have demonstrated a strong affinity for albumin in support of the hypothesis that exogenous lipids can be utilized by glioblastoma cells (18).

A soluble form of hydroxycitrate, a competitive inhibitor of ACLY, was used to assess ACLY's functional role in glycolysis *in vitro*. Hydroxycitrate is derived from the fruit of *Garcinia cambogia* and other *Garcinia* species. Hydroxycitrate is poorly absorbed and is required in relatively large amounts to compete with endogenous citric acid. Studies have shown that humans can safely ingest 13.5 g of hydroxycitrate per day with plasma levels of 82 mg/L (0.39 mM) achieved (62,63), and it has been shown to cross the blood brain barrier in rats to some extent (64). Although poor absorption and the high levels required for competition with citric acid limit the usefulness of hydroxycitrate, the functional results demonstrated here justify future development of non-competitive inhibitors with specificity for ACLY. Combining citric acid in with hydroxycitrate was not studied here in view of the potential for competition to occur at cell membrane tricarboxylate transporters but should also be considered.

Another inhibitor, radicicol, also suppressed cell migration with specificity for glycolytic conditions. This effect was attributed, at least in part, to radicicol's effect on ACLY, whereas its weaker effect on migration under normal conditions was attributed to its inhibition of HSP90. Decreased and increased levels of HSP90 and ACLY, respectively, in pseudopodia were consistent with attributing radicicol's effects on the leading edge of glycolytic migrating cells to its suppression of ACLY.

Clinical relevance for ACLY's role in brain tumor invasion was indicated by detection of increased ACLY in the pseudopodia formed by primary glioblastoma cells aspirated from a fresh tumor. Moreover, we detected significantly decreased survival among glioma patients who had increased expression of *ACLY* in the REMBRANDT database as well as a correlation between levels of *ACLY* and *ENO1* that encodes a key glycolytic enzyme, enolase 1.

In summary, our data support ACLY as a newly identified positive regulator of glycolysis in glioblastomas that can be targeted to suppress hypoxic cell migration and invasion (Fig. 8). Thus, ACLY serves as not only a target in oxygenated cells for suppression of lipid synthesis and histone acetylation, as shown by others, but also as a susceptible target in hypoxic cells to restore inhibition of glycolysis, as shown in these studies. The enhanced pseudopodial distribution of ACLY, association of its increased gene expression with decreased survival in glioma patients, strong association of increased *ACLY* expression with that of *ENO1* in gliomas and glioblastomas and ACLY's participation in tumor cell migration, clone formation and invasion are all findings that support ACLY as a positive regulator of glycolysis in glioblastoma cells. Overexpression of ACLY in non-small cell lung carcinoma and hepatocellular carcinoma compared to normal parenchyma has also been reported (65,66), suggesting that ACLY may represent a common target among highly malignant tumors. Furthermore, targeting glycolytic adaptations in brain tumor cells, such as increased levels of ACLY, is a therapeutic metabolic strategy that can be combined with other treatments, in keeping with results obtained for a similar strategy in several other types of malignant tumors (67–70). These studies suggest that suppression of glycolysis via inhibition of ACLY is functionally effective and sensitizes glioblastoma cells to non-metabolic inhibitors when mitochondrial function is impaired. This approach to inhibit hypoxic tumor cells would potentially complement anti-angiogenesis therapies that compromise the blood supply to tumor cells.

Acknowledgments

We acknowledge the Repository of Molecular for Brain Neoplasia Database (REMBRANDT) created and maintained by the NINDS, NCI, at the NIH for the availability of information on *ACLY* and *ENO1*. We thank Douglas E. Moul, MD, MPH, Department of Psychiatry, University of Pittsburgh, Pittsburgh, PA (relocated to Departments of Psychiatry and Neurology, Louisiana State University Health Sciences Center-Shreveport) for statistical advice. We thank The Michigan Proteome Consortium, University of Michigan, Ann Arbor, MI, and Melissa Melan, PhD and J.E. Dipaola, Department of Pathology, University of Pittsburgh, for technical assistance. We thank Ronald L. Hamilton, MD, and Colleen Lovell with the University of Pittsburgh Brain Bank with the cooperation of D. L. Lunsford, MD, for provision of primary brain tumor cells and tissue. We thank The Nick Eric Wichman Foundation, The Beez Foundation, and The Walter L. Copeland Fund for Cranial Research of The Pittsburgh Foundation (D2006-0379) for their support. Funding was also provided by NIH P01-NS40923 and by TATRC/Department of Defense, USAMRAA Prime Award W81XWH-05-2-0066.

Abbreviations

17-AAG	17-allylamino-17-demethoxygeldanamycin
AMPK	AMP-activated protein kinase
ACLY	ATP citrate lyase
BSA	bovine serum albumin
CM-DiI	chloromethyl derivative of 1,1’-dioctadecyl-3,3,3’,3’-tetramethylindocarbocyanine
CIs	confidence intervals
ddC_t	delta-delta crossing threshold
DP	digestion product
ENO1	enolase 1
FBS	fetal bovine serum
GAPDH	glyceraldehyde-3-phosphate dehydrogenase
HSP90	heat shock protein 90
H&E	hematoxylin and eosin
HGF	hepatocyte growth factor
IC_{50}’s	inhibitory concentrations for 50% suppression compared to controls
IRB	Institutional Review Board
MALDI-TOF-MS	matrix-assisted laser desorption ionization time-of-flight mass spectrometry
M_r	molecular weight
1D	one-dimensional
MEM	Minimal Essential Medium
NCBI	National Center for Biotechnology Information
p	phosphorylated
pI	isoelectric point
Ps	pseudopodia
RQ-PCR	real-time quantitative polymerase chain reaction
REMBRANDT	Repository of Molecular Brain Neoplasia Database

2D	two-dimensional
UC	unmigrated cells

References

1. Oudard S, Arvelo F, Miccoli L, Apiou F, Dutrillaux AM, Poisson M, Dutrillaux B, Poupon MF. High glycolysis in gliomas despite low hexokinase transcription and activity correlated to chromosome 10 loss. Br J Cancer. 1996; 74:839–845. [PubMed: 8826847]
2. Oudard S, Boitier E, Miccoli L, Rousset S, Dutrillaux B, Poupon MF. Gliomas are driven by glycolysis: putative roles of hexokinase, oxidative phosphorylation and mitochondrial ultrastructure. Anticancer Res. 1997; 17:1903–1911. [PubMed: 9216643]
3. Vaupel P, Kallinowski F, Okunieff P. Blood flow, oxygen and nutrient supply, and metabolic microenvironment of human tumors: a review. Cancer Res. 1989; 49:6449–6465. [PubMed: 2684393]
4. Beckner ME, Stracke ML, Liotta LA, Schiffmann E. Glycolysis as primary energy source in tumor cell chemotaxis. J Natl Cancer Inst. 1990; 82:1836–1840. [PubMed: 2174462]
5. Beckner ME, Gobbel GT, Abounader R, Burovic F, Agostino NR, Laterra J, Pollack IF. Glycolytic glioma cells with active glycogen synthase are sensitive to PTEN and inhibitors of PI3K and gluconeogenesis. Lab Invest. 2005; 85:316–325. [PubMed: 15654357]
6. Beckner ME, Chen X, An J, Day BW, Pollack IF. Proteomic characterization of harvested pseudopodia with differential gel electrophoresis and specific antibodies. Lab Invest. 2005; 85:316–327. [PubMed: 15654357]
7. Repository of Molecular Brain Neoplasia Database (REMBRANDT) v1.5.2, generated and maintained by the NCI and NINDS at NIH. [February, 2009 data]. http://rembrandt.nci.nih.gov
8. Srere PA. The citrate cleavage enzyme. I. Distribution and purification. J Biol Chem. 1959; 234:2544–2547. [PubMed: 13833535]
9. Rafalowska U. Transport of malate and citrate into rat brain mitochondria under hypoxia and anesthesia. Neurochem Res. 1979; 4:355–364. [PubMed: 460527]
10. Lowry OH, Passonneau JV. The application of quantitative histochemistry to the pharmacology of the nervous system. Biochem Pharmacol. 1962; 9:173–180. [PubMed: 13931306]
11. Szutowicz A, Stepien M, Lysiak W, Angielski S. Effect of (−)-hydroxycitrate on the activities of ATP citrate lyase and the enzymes of acetyl-CoA metabolism in rat brain. Acta Biochim Pol. 1976; 23:227–234. [PubMed: 970036]
12. Tornheim K, Lowenstein JM. Control of phosphofructokinase from rat skeletal muscle. J Biol Chem. 1976; 251:7322–7328. [PubMed: 12161]
13. Likavconova K, Dobrota D, Liptaj T, Pronayova N, Mlynarik V, Belan V, Galanda M, Beres A, De Riggo J. In vitro study of astrocytic tumour metabolism by proton magnetic resonance spectroscopy. Gen Physiol Biophys. 2005; 24:327–335. [PubMed: 16308427]
14. Brockmann MA, Ulbricht U, Gruner K, Fillbrandt R, Westphal M, Lamszus K. Glioblastoma and cerebral microvascular endothelial cell migration in response to tumor-associated growth factors. Neurosurgery. 2003; 52:1391–1399. discussion 1399. [PubMed: 12762884]
15. Ki SW, Ishigami K, Kitahara T, Kasahara K, Yoshida M, Horinouchi S. Radicicol binds and inhibits mammalian ATP citrate lyase. J Biol Chem. 2000; 275:39231–39236. [PubMed: 11007781]
16. Beckner ME, Jane EP, Jankowitz B, Agostino NR, Walter KA, Hamilton RL, Pollack IF. Tumor cells from ultrasonic aspirations of glioblastomas migrate and form spheres with radial outgrowth. Cancer Lett. 2007; 255:135–144. [PubMed: 17543444]
17. Said HM, Hagemann C, Stojic J, Schoemig B, Vince GH, Flentje M, Roosen K, Vordermark D. GAPDH is not regulated in human glioblastoma under hypoxic conditions. BMC Molec Biol. 2007; 8:55. Doi:10.1186/1471-2199-8-55. [PubMed: 17597534]

18. Beckner ME, Zhang Z, Agostino NR, Day BW, Pollack IF. Albumin marks pseudopodia of astrocytoma cells responding to hepatocyte growth factor or serum. Lab Invest. 2006; 86:1103–1114. [PubMed: 16969371]
19. Dringen R, Gebhardt R, Hamprecht B. Glycogen in astrocytes: possible function as lactate supply for neighboring cells. Brain Res. 1993; 623:208–214. [PubMed: 8221102]
20. Rose CR, Waxman SG, Ransom BR. Effects of glucose deprivation, chemical hypoxia, and simulated ischemia on Na+ homeostasis in rat spinal cord astrocytes. J Neurosci. 1998; 18:3554–3562. [PubMed: 9570787]
21. Swanson RA, Benington JH. Astrocyte glucose metabolism under normal and pathological conditions *in vitro*. Dev Neurosci. 1996; 18:515–521. [PubMed: 8940626]
22. Bennett MC, Diamond DM, Stryker SL, Parks JK, Parker WD Jr. Cytochrome oxidase inhibition: a novel animal model of Alzheimer's disease. J Geriatr Psychiatry Neurol. 1992; 5:93–101. [PubMed: 1317179]
23. Bennett MC, Mlady GW, Fleshner M, Rose GM. Synergy between chronic corticosterone and sodium azide treatments in producing a spatial learning deficit and inhibiting cytochrome oxidase activity. Proc Natl Acad Sci USA. 1996; 93:1330–1334. [PubMed: 8577764]
24. Bennett MC, Mlady GW, Kwon YH, Rose GM. Chronic *in vivo* sodium azide infusion induces selective and stable inhibition of cytochrome *c* oxidase. J Neurochem. 1996; 66:2606–2611. [PubMed: 8632188]
25. Knyihar-Csillik E, Okuno E, Vecsei L. Effects of in vivo sodium azide administration on the immunohistochemical localization of kynurenine aminotransferase in the rat brain. Neuroscience. 1999; 94:269–277. [PubMed: 10613517]
26. Berndt JD, Callaway NL, Gonzalez-Lima F. Effects of chronic sodium azide on brain and muscle cytochrome oxidase activity: a potential model to investigate environmental contributions to neurodegenerative diseases. J Toxicol Environ Health A. 2001; 63:67–77. [PubMed: 11346134]
27. Zhu M, Li M-w, Tian X-s, Ou X-m, Zhu C-q, Guo J-c. Neuroprotective role of δ-opiod receptors against mitochondrial respiratory chain injury. Brain Research. 2009; 1252:183–191. [PubMed: 19056363]
28. Selvatici R, Previati M, Marino S, Marani L, Falzarano S, Lanzoni I, Siniscalchi A. Sodium azide induced neuronal damage in vitro: evidence for non-apoptotic cell death. Neurochem Res. 2009; 34:909–916. [PubMed: 18841470]
29. Bagetta V, Barone I, Ghiglieri V, Di Filippo M, Sgobio C, Bernardi G, Calbresi P, Picconi B. Acetyl-L-carnitine selectively prevents post-ischemic LTP via a possible action on mitochondrial energy metabolism. Neuropharmacol. 2008; 55:223–229.
30. Lill U, Schreil A, Eggerer H. Isolation of enzymically active fragments formed by limited proteolysis of ATP citrate lyase. Eur J Biochem. 1982; 125:645–650. [PubMed: 6749502]
31. Singh M, Richards EG, Mukherjee A, Srere PA. Structure of ATP citrate lyase from rat liver. Physicochemical studies and proteolytic modification. J Biol Chem. 1976; 251:5242–5250. [PubMed: 821950]
32. Preuss HG, Bagchi D, Bagchi M, Rao CV, Dey DK, Satyanarayana S. Effects of natural extract of (−)-hydroxycitric acid (HCA-SX) and a combination of HCA-SX plus niacin-bound chromium and *Gymnema sylvestre* extract on weight loss. Diabetes Obes Metab. 2004; 6:171–180. [PubMed: 15056124]
33. Neckers L. Using natural product inhibitors to validate Hsp90 as a molecular target in cancer. Curr Top Med Chem. 2006; 6:1163. [PubMed: 16842153]
34. Price JT, Quinn JMW, Sims NA, Vieusseaux J, Waldeck K, Docherty SE, Myers D, Nakamura A, Waltham MC, Gillespie MT, Thompson EW. The heat shock protein 90 inhibitor, 17-allylamino-17-demethoxygeldanamycin, enhances osteoclast formation and potentiates bone metastasis of a human breast cancer cell line. Cancer Res. 2005; 65:4929–4938. [PubMed: 15930315]
35. Berthou S, Aebersold DM, Schmidt LS, Stroka D, Heigl C, Streit B, Stalder D, Gruber G, Liang C, Howlett AR, Candinas D, Greiner RH, et al. The Met kinase inhibitor SU11274 exhibits a selective inhibition pattern toward different receptor mutated variants. Oncogene. 2004; 23:5387–5393. [PubMed: 15064724]

36. Ma PC, Jagadeeswaran R, Jagadeesh S, Tretiakova MS, Nallasura V, Fox EA, Hansen M, Schaefer E, Naoki K, Lader A, Richards W, Sugarbaker D, et al. Functional expression and mutations of c-Met and its therapeutic inhibition with SU11274 and small interfering RNA in non-small cell lung cancer. Cancer Res. 2005; 65:1479–1488. [PubMed: 15735036]
37. Li H, Jiang T, Lin Y, Zhao Z, Zhang N. HGF protects rat mesangial cells from high-glucose-mediated oxidative stress. Am J Nephrol. 2006; 26:519–530. [PubMed: 17124385]
38. Puri N, Ahmed S, Janamanchi V, Tretiakova M, Zumba O, Krausz T, Jagadeeswaran R, Salgia R. c-Met is a potentially new therapeutic target for treatment of human melanoma. Clin Cancer Res. 2007; 13:2246–2253. [PubMed: 17404109]
39. Patel TB, Clark JB. Lipogenesis in the brain of suckling rats. Studies on the mechanism of mitochondrial-cytosolic carbon transfer. Biochm J. 1980; 188:163–168.
40. Sonnewald U, Westergaard N, Krane J, Unsgard G, Petersen SB, Schousboe A. First direct demonstration of preferential release of citrate from astrocytes using [13C]NMR spectroscopy of cultured neurons and astrocytes. Neurosci Lett. 1991; 128:235–239. [PubMed: 1945042]
41. Waagepetersen HS, Sonnewald U, Larsson OM, Schousboe A. Multiple compartments with different metabolic characteristics are involved in biosynthesis of intracellular and released glutamine and citrate in astrocytes. Glia. 2001; 35:246–252. [PubMed: 11494415]
42. Parlo RA, Coleman PS. Enhanced rate of citrate export from cholesterol-rich hepatoma mitochondria. The truncated Krebs cycle and other metabolic ramifications of mitochondrial membrane cholesterol. J Biol Chem. 1984; 259:9997–10003. [PubMed: 6469976]
43. Lowry OH, Berger SJ, Carater JG, Chi MM, Manchester JK, Knor J, Pusateri ME. Diversity of metabolic patterns in human brain tumors: enzymes of energy metabolism and related metabolites and cofactors. J Neurochem. 1983; 41:994–1010. [PubMed: 6619861]
44. Seymour ZA, Panigrahy A, Finlay JL, Nelson MD, Bluml S. Citrate in pediatric CNS tumors? AJNR Am J Neuroradiol. 2008; 29:1006–1011. [PubMed: 18272551]
45. Brat DJ, Castellano-Sanchez AA, Hunter SB, Pecot M, Cohen C, Hammond EH, Devi SN, Kaur B, Van Meir EG. Pseudopalisades in glioblastoma are hypoxic, express extracellular matrix proteases, and are formed by an actively migrating cell population. Cancer Res. 2004; 64:920–927. [PubMed: 14871821]
46. Brat DJ, Van Meir EG. Vaso-occlusive and prothrombotic mechanisms associated with tumor hypoxia, necrosis, and accelerated growth in glioblastoma. Lab Invest. 2004; 84:397–405. [PubMed: 14990981]
47. Sakata K, Kwok TT, Murphy BJ, Laderoute KR, Gordon GR, Sutherland RM. Hypoxia-induced drug resistance: comparison to P-glycoprotein-associated drug resistance. Br J Cancer. 1991; 64:809–814. [PubMed: 1681885]
48. Yamauchi T, Raffin TA, Yang P, Sikic BI. Differential protective effects of varying degrees of hypoxia on the cytotoxicities of etoposide and bleomycin. Cancer Chemother Pharmacol. 1987; 19:282–286. [PubMed: 2439223]
49. Gupta V, Costanzi JJ. Role of hypoxia in anticancer drug-induced cytotoxicity for Ehrlich ascites cells. Cancer Res. 1987; 47:2407–2412. [PubMed: 2436764]
50. Wilson RE, Keng PC, Sutherland RM. Drug resistance in Chinese hamster ovary cells during recovery from severe hypoxia. J Natl Cancer Inst. 1989; 81:1235–1240. [PubMed: 2474076]
51. Luk CK, Veinot-Drebot L, Tjan E, Tannock IF. Effect of transient hypoxia on sensitivity to doxorubicin in human and murine cell lines. J Natl Cancer Inst. 1990; 82:684–692. [PubMed: 1969493]
52. Song X, Liu X, Chi W, Liu Y, Wei L, Wang X, Yu J. Hypoxia-induced resistance to cisplatin and doxorubicin in non-small cell lung cancer is inhibited by silencing of HIF-1alpha gene. Cancer Chemother Pharmacol. 2006; 58:776–784. [PubMed: 16532342]
53. Sanna K, Rofstad EK. Hypoxia-induced resistance to doxorubicin and methotrexate in human melanoma cell lines in vitro. Int J Cancer. 1994; 58:258–262. [PubMed: 8026888]
54. DeHaan C, Habibi-Nazhad B, Yan E, Salloum N, Parliament M, Allalunis-Turner J. Mutation in mitochondrial complex I ND6 subunit is associated with defective response to hypoxia in human glioma cells. Mol Cancer. 2004; 3:19. [PubMed: 15248896]

55. Beckner ME, Gleixner SL, Pollack IF. STI571's inhibition of spontaneous cell motility in Boyden chambers shows specificity for cell type and non-hypoxic conditions. Proc Am Assoc Cancer Res. 2002; 43:1084.
56. Pfeiffer T, Schuster S, Bonhoeffer S. Cooperation and competition in the evolution of ATP-producing pathways. Science. 2001; 292:504–507. [PubMed: 11283355]
57. Hatzivassiliou G, Zhao F, Bauer DE, Andreadis C, Shaw AN, Dhanak D, Hingorani SR, Tuveson DA, Thompson CB. ATP citrate lyase inhibition can suppress tumor cell growth. Cancer Cell. 2005; 8:311–321. [PubMed: 16226706]
58. Wellen KE, Hatzivassiliou G, Sachdeva UM, Bui TV, Cross JR, Thompson CB. ATP-citrate lyase links cellular metabolism to histone acetylation. Science. 2009; 324:1076–1080. [PubMed: 19461003]
59. Wang Y, Karu K, Griffiths WJ. Analysis of neurosterols and neurosteroids by mass spectrometry. Biochimie. 2007; 89:182–191. [PubMed: 17126470]
60. Spector AA. Plasma free fatty acid and lipoproteins as sources of polyunsaturated fatty acid for the brain. J Mol Neurosci. 2001; 16:159–165. [PubMed: 11478370]
61. Swinnen JV, Beckers A, Brusselmans K, Organe S, Segers J, Timmermans L, Vanderhoydonc F, Deboel L, Derua R, Waelkens E, De Schrijver E, Van de Sande T, et al. Mimicry of a cellular low energy status blocks tumor cell anabolism and suppresses the malignant phenotype. Cancer Res. 2005; 65:2441–2448. [PubMed: 15781660]
62. Downs BW, Bagchi M, Subbaraju GV, Shara MA, Preuss HG, Bagchi D. Bioefficacy of a novel calcium-potassium salt of (−)-hydroxycitric acid. Mutat Res. 2005; 579:149–162. [PubMed: 16055158]
63. van Loon LJ, van Rooijen JJ, Niesen B, Verhagen H, Saris WH, Wagenmakers AJ. Effects of acute (−)-hydroxycitrate supplementation on substrate metabolism at rest and during exercise in humans. Am J Clin Nutr. 2000; 72:1445–1450. [PubMed: 11101469]
64. Ohia SE, Opere CA, LeDay AM, Bagchi M, Bagchi D, Stohs SJ. Safety and mechanism of appetite suppression by a novel hydroxycitric acid extract (HCA-SX). Mol Cell Biochem. 2002; 238:89–103. [PubMed: 12349913]
65. Migita T, Narita T, Nomura K, Miyagi E, Inazuka F, Matsuura M, Ushijima, Mashima T, Seimiya H, Satoh Y, Okumura S, Nakagawa K, Ishikawa Y. ATP citrate lyase: Activation and therapeutic implications in non-small cell lung cancer. Cancer Res. 2008; 68:8547–8554. [PubMed: 18922930]
66. Yahagi N, Shimano H, Hasegawa K, Ohashi K, Matsuzaka T, Najima Y, Sekiya M, Tomita S, Okazaki H, Tamura Y, Iizuka Y, Ohashi K, et al. o-ordinate activation of lipogenic enzymes in hepatocellular carcinoma. Eur J Cancer. 2005; 41:1316–1322. [PubMed: 15869874]
67. Simons AL, Ahmad IM, Mattson DM, Dornfeld KJ, Spitz DR. 2-Deoxy-d-glucose combined with cisplatin enhances cytotoxicity via metabolic oxidative stress in human head and neck cancer cells. Cancer Res. 2007; 67:3364–3370. [PubMed: 17409446]
68. Colofiore JR, Stolfi RL, Nord LD, Martin DS. Biochemical modulation of tumor cell energy. IV. Evidence for the contribution of adenosine triphosphate (ATP) depletion to chemotherapeutically-induced tumor regression. Biochem Pharmacol. 1995; 50:1943–1948. [PubMed: 8615876]
69. Martin DS, Bertino JR, Koutcher JA. ATP depletion + pyrimidine depletion can markedly enhance cancer therapy: fresh insight for a new approach. Cancer Res. 2000; 60:6776–6783. [PubMed: 11156364]
70. Maschek G, Savaraj N, Priebe W, Braunschweiger P, Hamilton K, Tidmarsh GF, De Young LR, Lampidis TJ. 2-Deoxy-d-glucose increases the efficacy of adriamycin and paclitaxel in human osteosarcoma and non-small cell lung cancers *in vivo*. Cancer Res. 2004; 64:31–34. [PubMed: 14729604]

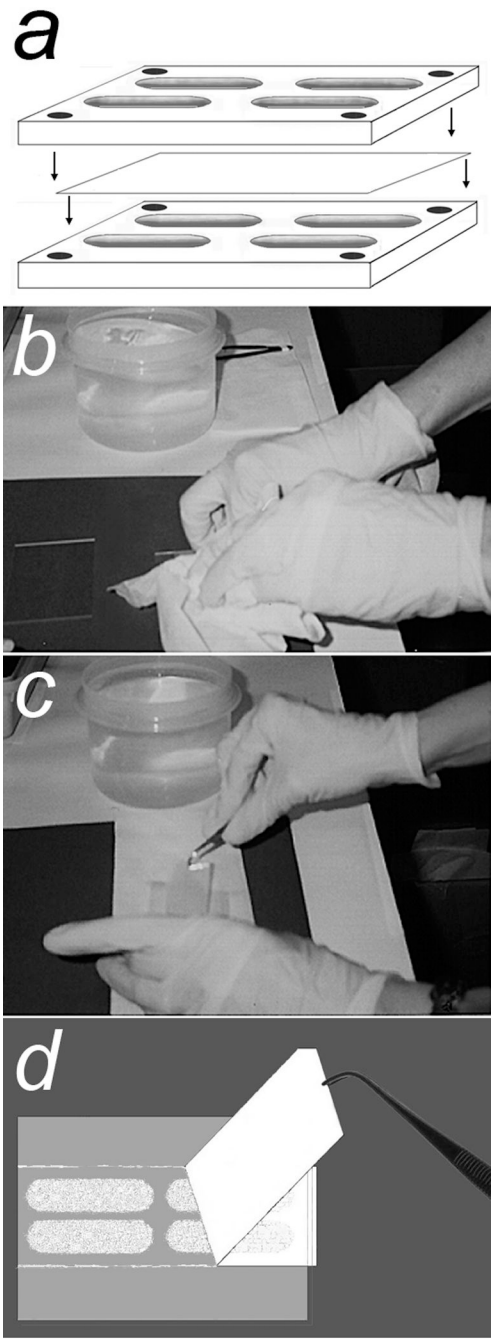

Figure 1.

Procedure for retrieval of pseudopodia from Boyden chamber filters. *a*. A Boyden chamber with four large wells was assembled with a gelatin coated filter (containing 3 or 1 μm pores) separating top and bottom wells. Chemoattractants were present in the bottom wells. Single cell suspensions were added to the top wells. *b*. After a 6 h incubation in cell culture conditions, the filter was removed and submerged in 100% methanol for 30 s. The filter was placed on a glass slide with unmigrated cell materials on the top surface. This material was gently wiped away completely with minimal pressure using large Kimwipes. Fresh Kimwipes were then used to apply firm pressure for 30 s to force adherence of pseudopodia

to the glass. *c*. and *d*. The filter was then carefully peeled off while leaving behind pseudopodia adherent to the glass.

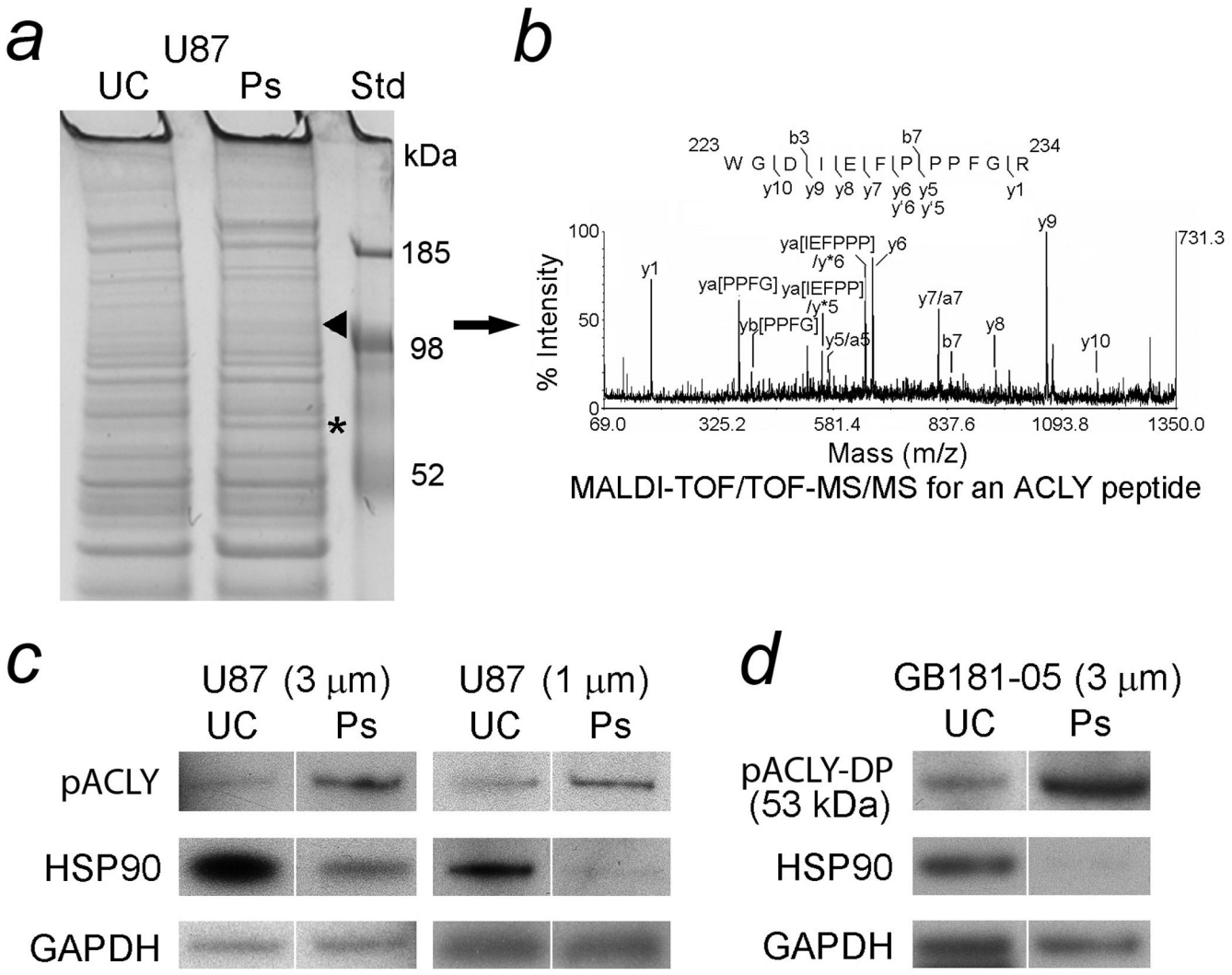

Figure 2.

Identification of increased proteins in lysates of glioblastoma pseudopodia (Ps) compared to unmigrated cells (UC). Cells extended Ps through filters in Boyden migration chambers in response to chemoattractants (FBS and HGF) that were then harvested as pseudopodial lysates. UC from the opposite side of the filters were also harvested in a similar manner. *a*. Lysates of U87 glioblastoma cells demonstrated increased bands, 121 kDa (arrowhead) and 68 kDa (asterisk), in Ps formed on filters containing 3-μm diameter pores compared to UC. The bands were submitted for trypsin digestion and identification with mass spectrometry (MS). The increased 121 and 68 kDa bands in lysates of Ps were ATP citrate lyase (ACLY) and bovine serum albumin (BSA), respectively. Identification of increased BSA in the lysates of glioblastoma Ps has been described (25). *b*. The MALDI-TOF/TOF-MS/MS spectrum for an ACLY peptide with a $[M + H]^+$ precursor ion of mass/charge (*m/z*) ratio 1417.67. Tryptic digestion of the 121 kDa band included a match for the peptide sequence ^{223}WGDIEFPPPFGR^{234} (ion score = 153, derived from ACLY isoform 2 [*Homo sapiens*]. *c*. The Ps of U87 cells demonstrated increased immunoreactivity for pACLY (125 kDa), 3.50-fold and 2.38-fold, respectively, when filters with 3- and 1-μm diameter pores were used for their formation. The levels of heat shock protein (HSP) 90 (92 KDa) in Ps (3- and 1-μm) fell to 46% and 39%, respectively, compared to the levels in UC. To demonstrate

equalized loading, the levels of GAPDH (36 kDa) in lysates of Ps (3- and 1-μm) were 91% and 95%, respectively, of the levels in UC and the levels of total protein were also similar. *d*. ACLY was also compared in immunoblots of freshly aspirated primary glioblastoma cells and their Ps. The molecular weight of the immunoreactive band (53 kDa) that reacted with anti-pACLY was the same as an established proteolytic digestion product of ACLY (ACLY-DP) that is known to retain activity (30,31). The levels of pACLY-DP were 4.69-fold greater in lysates of the Ps formed by primary cells than lysates of UC. The levels of HSP90 in the primary cell Ps were only 7% of their levels in UC. Loading was approximately equalized with GAPDH at levels in the Ps formed by primary cells that were 84% of those in UC.

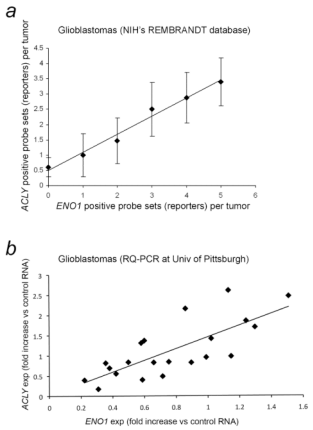

Figure 3.

Concordant expression of *ACLY* with *ENO1* that encodes enolase, a glycolytic enzyme. *a*. The relationships for gene expression of *ACLY* and *ENO1* in 109 glioblastomas found in NIH's REMBRANDT v1.5.2 brain tumor database (7). The mean number of probe sets (reporters) with 95% CI indicating increased expression of *ACLY* are graphed on the y axis against the number of probe sets indicating increased expression of *ENO1* in each glioblastoma on the×axis. A trendline is included. As the number of probe sets for at least two-fold increased expression of *ENO1* increased from zero to five in each glioblastoma, the numbers of probe sets for increased expression of *ACLY* increased concordantly from zero to four. The correlation coefficient (*r*) is 0.990, $p < 0.00005$. *b*. The fold changes in expression levels of *ACLY* and *ENO1* compared to pooled reference RNA from non-malignant brain tissue (multiple brain regions combined) were determined with RQ-PCR of frozen tissue from 22 glioblastoma resections using the ddC_t method. Normalization was achieved via two housekeeping genes, *ACTB* and *GAPDH*. One outlier was discarded (see text). The correlations of fold-changes in gene expressions for *ACLY* and *ENO1* (compared to the pooled reference RNA) in 21 brain tumors are graphed with a trendline included. The *r* for fold changes in expression of *ACLY* and *ENO1* is 0.756, $p < 0.0001$. No differences were found in the C_ts of controls for tumor and reference samples ($p < 0.05$ level of significance) in regard to human genomic DNA contamination and reverse transcription. Expression = exp, RQ-PCR = real-time quantitative PCR.

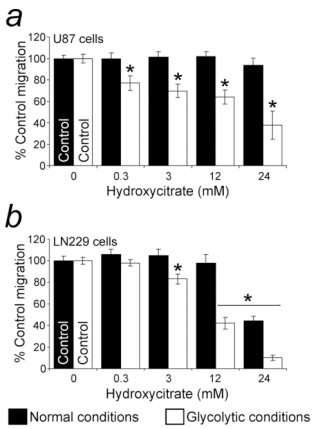

Figure 4.

Inhibition of glioblastoma cell migration with inhibition of ACLY by hydroxycitrate. *a*. Inhibition of U87 cell migration with hydroxycitrate, a competitive inhibitor of ACLY. Glycolytic conditions were generated by adding NaN_3 (27 mM) to suppress mitochondrial respiration. A water-soluble form of hydroxycitrate suppressed glycolytic migration in concentrations of 0.3 mM without suppressing the migration in normal conditions compared to control levels (no drug). *b*. Inhibition of migration by LN229 cells, another glioblastoma cell line, with hydroxycitrate. Concentrations of 3 mM hydroxycitrate suppressed glycolytic migration. Migration in normal conditions (without mitochondrial inhibition) was suppressed by hydroxycitrate at 24 mM. Cell viability was maintained for the length of the assays. Significant ($p < 0.05$) differences compared to the migration of control cells (no hydroxycitrate) are indicated by asterisks (*).

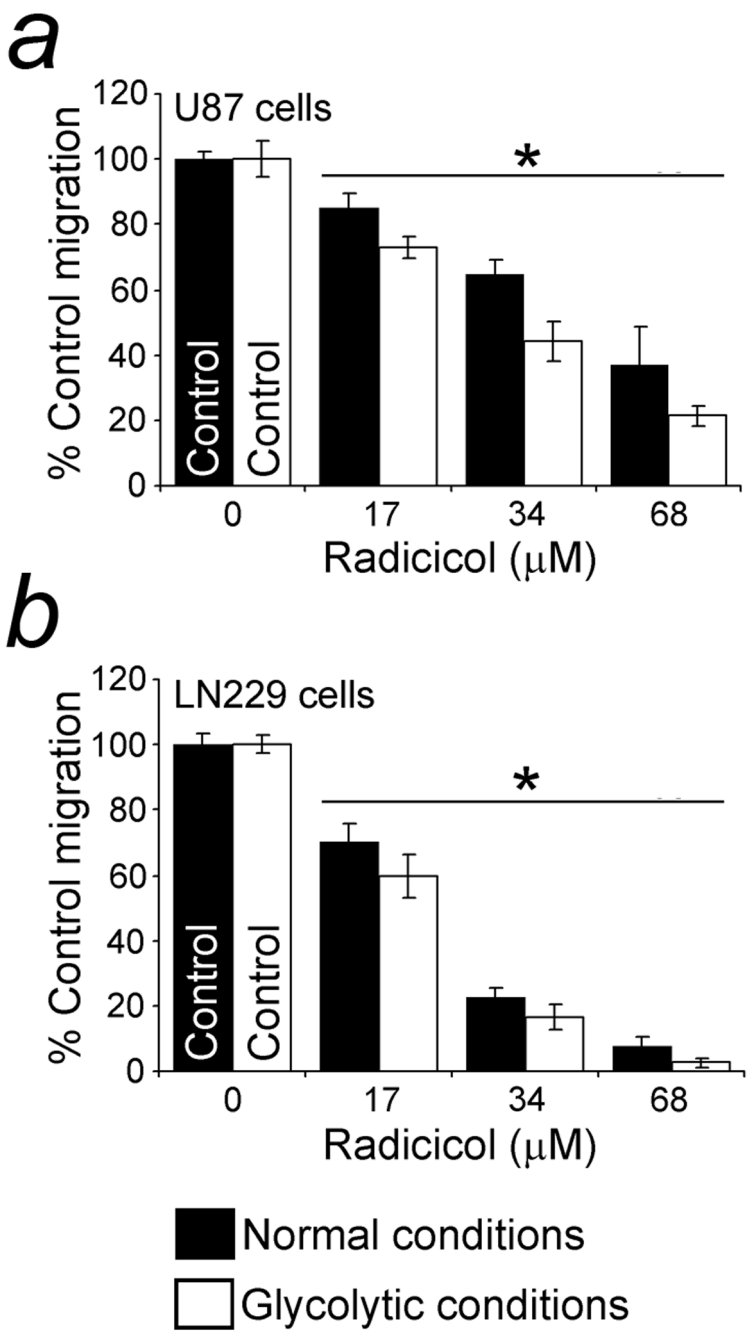

Figure 5.

Suppression of cell migration with inhibition of ACLY by radicicol. *a*. Suppression of U87 migration with radicicol, another inhibitor of ACLY (15) that also inhibits HSP90. Radicicol, 17 μM, suppressed migration, with and without a mitochondrial inhibitor present. Since Met and many other kinases are chaperoned by HSP90, a suppressive effect on cell migration via HSP90 was multifaceted and less specific for glycolytic conditions. *b*. Suppression of LN229 migration by radicicol, with and without mitochondrial inhibition. Migration was significantly inhibited by radicicol at 17 μM. Cell viability was maintained for the length of the assays. Significant ($p < 0.05$) differences from the migration of control cells (no drug) are indicated by asterisks (*).

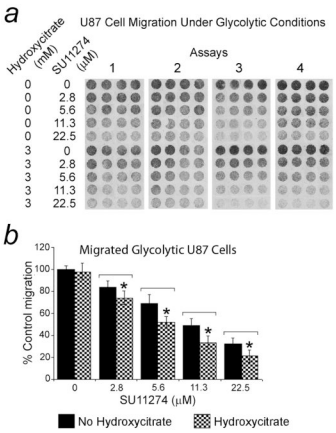

Figure 6.

Hydroxycitrate enhanced suppression of glioblastoma cell migration by SU11274 under glycolytic conditions. The Met kinase inhibitor, SU11274, inhibited migration of U87 cells significantly with a dose response. Hydroxycitrate (3 mM) combined with SU11274 (2.8 – 22.5 μM) showed a significant ($p < 0.05$) additive suppressive effect. *a*. Migrated U87 cell pellets (3 mm diameter). *b*. Graph of averaged cell migration results for the dose curves. In four assays, the IC_{50} of SU11274 for U87 cells, 14.2 μM, was reduced to 7.47 μM when 3 mM hydroxycitrate was present. Results are stated as the mean percent of control migration (no hydroxycitrate or SU11274) with 95% CIs.

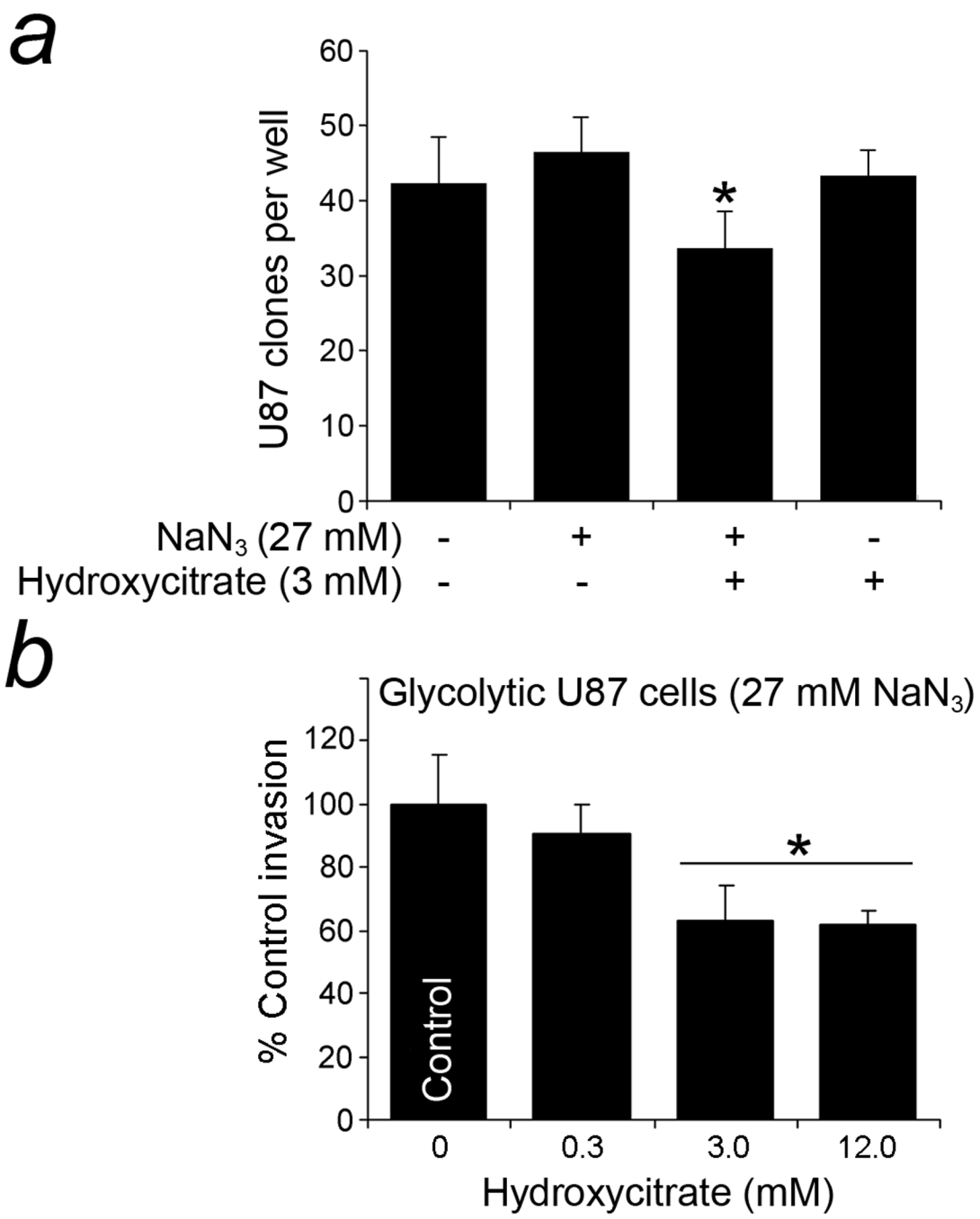

Figure 7.

Suppression of other types of functional assays (clonogenicity and invasion) with an inhibitor of ACLY in glycolytic U87 cells. *a*. Suppression of the clonogenic potential in glycolytic U87 cells with inhibition of ACLY. Hydroxycitrate suppressed the clonogenic potential of U87 cells that had been forced to be transiently glycolytic via exposure to 27 mM NaN_3 for 5 h prior to being plated in culture for 10 days. Exposure to only hydroxycitrate or glycolytic conditions generated by NaN_3 without hydroxycitrate present did not suppress the clonogenic potential of U87 cells. However, in the presence of 3 mM hydroxcitrate, the cells that had been exposed to glycolytic conditions (NaN_3 present) prior to plating were significantly impaired in their clonogenic potential compared either to cells

unexposed to hydroxycitrate or NaN_3, $p < 0.05$, or to cells exposed to NaN_3 alone, $p < 0.001$, as indicated by the asterisk (*). *b*. Suppression of glioblastoma invasion in rat brain slices by inhibition of ACLY. Hydroxycitrate, 3 and 12 mM, suppressed invading U87 cells at a significance level of $p < 0.05$, as indicated by the asterisk (*). Under glycolytic conditions (27 mM NaN_3 present), cells labeled with CM-DiI were immobilized in solidified Matrigel on surfaces of sliced rat brain in a two well system with gradients of chemoattractants gradients (FBS and HGF). Hydroxycitrate, in concentrations indicated, was added on both sides of the brain slices. After 7 d in routine culture, histological sections were examined to count labeled cells at the bottom edges of brain slices. The average cell counts, expressed as percent of control invasion (no hydroxycitrate), with 95% CIs are shown.

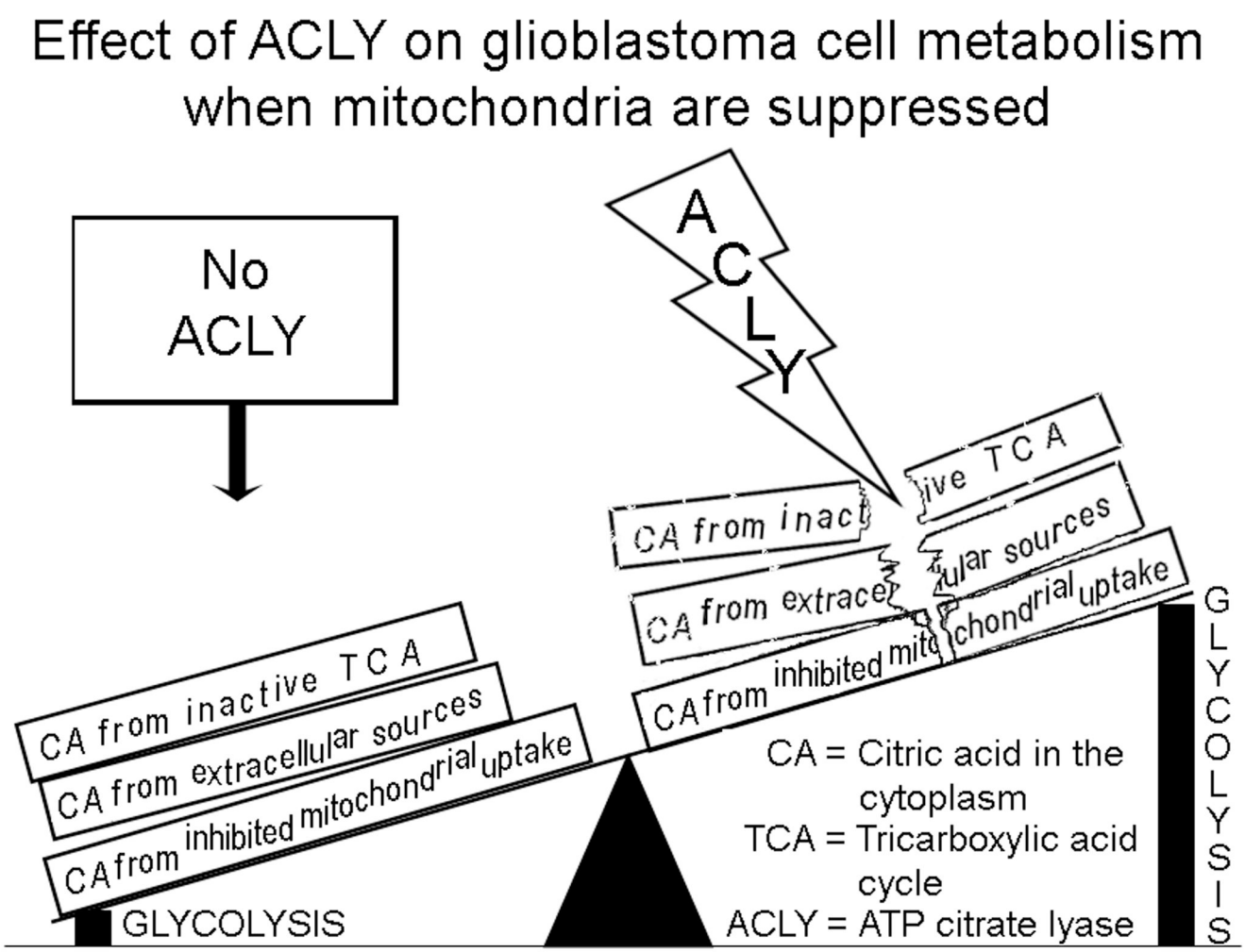

Figure 8.

Theory to explain the effect of ACLY on glioblastoma cells under conditions that suppress mitochondrial production of ATP. Mitochondria can be dysfunctional due to hypoxia, ischemia, genetic instability, drug effects, toxin effects, etc. In hypoxia, mitochondrial uptake of cytosolic citric acid is impaired (9). Accumulation of citric acid in the cytoplasm potentially inhibits glycolysis, whereas the cleavage activity of ACLY protects glycolysis from the inhibitory effects of citric acid. This may also occur regionally in pseudopodia directed away from the vasculature during invasive cell migration.

Table 1

Gene expression of *ENO1* and *ACLY* in the gliomas found in REMBRANDT v1. 5.2, a NIH database of brain tumors. Significantly decreased survival (Kaplan Meier) was associated with increased (at least two-fold) expression of either gene. Varying numbers of patients had increased gene expression according to the probe set (reporter) used. The total number of gliomas was 209. Results with Affymetrix (Affy.) and Unified Gene (U.G.) types of probe sets are listed. Unified Gene probe sets were derived from Affymetrix probe sets by according to NIH algorithms that selected probes with the best performances for each gene statistically. Within each type, the probe sets are ranked according to their highest overall mean intensity of signals. Data obtained in February, 2009.

ENO1					***ACLY***				
Affy.	**Probe sets (reporters)**	**# with ≥ 2X ↑exp**	**↓Survival (*p*) for ≥2X ↑exp**	**# with ≥ 2X ↓exp**	**Affy.**	**Probe sets (reporters)**	**# with ≥ 2X ↑exp**	**↓Survival (*p*) for ≥2X ↑exp**	**# with ≥ 2X ↓exp**
1st	201231_s_at	17	0.0057	3	1st	201128_s_at	41	0.0049	0
2nd	217294_s_at	29	0.0013	11	2nd	210337_s_at	80	0.018	6
3rd	240258_at	88	6.0×10^{-4}	36	3rd	201127_s_at	45	0.0014	0
U.G.					G				
1st	2023	34	0.0014	0	1st	47	52	8.0×10^{-4}	0
2nd	240258_at	44	0.0010	27	-	-	-	-	-

Int J Cancer. Author manuscript; available in PMC 2011 May 15.